Classical and quantum signatures of competing $\chi^{(2)}$ nonlinearities

A. G. White,[1] P. K. Lam,[1,*] M. S. Taubman,[1] M. A. M. Marte,[2] S. Schiller,[3] D. E. McClelland,[1] and H.-A. Bachor[1]

[1]*Physics Department, Australian National University, Canberra ACT 0200, Australia*
[2]*Institut für Physik, Universität Innsbruck, A-6020, Innsbruck, Austria*
[3]*Fakultät für Physik, Universität Konstanz, D78434, Konstanz, Germany*

We report the observation of the quantum effects of competing $\chi^{(2)}$ nonlinearities. We also report classical signatures of competition, namely, clamping of the second-harmonic power and production of nondegenerate frequencies in the visible. Theory is presented that describes the observations as resulting from competition between various $\chi^{(2)}$ up-conversion and down-conversion processes. We show that competition imposes hitherto unsuspected limits to both power generation and squeezing. The observed signatures are expected to be significant effects in practical systems. [S1050-2947(97)04406-5]

PACS number(s): 42.65.Ky, 03.65.Sq, 42.50.Dv, 42.79.Nv

Second-order, or $\chi^{(2)}$, nonlinear optical systems are employed successfully in applications ranging from frequency conversion to quantum optics. The four basic $\chi^{(2)}$ processes are second-harmonic and sum frequency generation (SHG and SFG, up-conversion); and difference frequency generation and (non)degenerate optical parametric oscillation (DFG or (N)DOPO, down-conversion). In recent years there has been increasing interest in the behavior of *interacting* $\chi^{(2)}$ nonlinearities.

Interacting nonlinearities can be categorized as *cooperating* and *competing*. Cooperating nonlinearities are those where all the down-conversion and up-conversion processes share the same modes, e.g., $\nu \rightleftharpoons 2\nu$ or $\nu \pm \Delta_1 \rightleftharpoons 2\nu$. Competing nonlinearities are those where all the down-conversion and up-conversion processes do not share the same modes, e.g., $\nu \rightleftharpoons 2\nu \rightleftharpoons \nu \pm \Delta_2$, or, $\nu \pm \Delta_1 \rightleftharpoons 2\nu \rightleftharpoons \nu \pm \Delta_2$. Both forms of interaction are often referred to as *cascaded* nonlinearities.

An early study of cooperating $\chi^{(2)}$ nonlinearities predicted power limiting of the pump in an optical parametric oscillator [1]. More recently the large third-order effects possible via cooperating $\chi^{(2)}$ nonlinearities has been the subject of extensive research [2,3], including continuous wave (CW) studies using cavities [4,5]. Systems of cooperating nonlinearities hold promise for applications including optical switching, nonlinear optical amplification [6], squeezing and quantum nondemolition (QND) measurements [4].

In contrast, systems of competing nonlinearities have been mainly investigated for their potential as frequency tunable sources of light. Systems considered include: intracavity SFG and NDOPO [7,8]; intracavity DFG and NDOPO [9]; and intracavity SHG and NDOPO [10–15]. The quantum properties of the latter system have been modeled for the quadruply resonant configuration [16] and several nonclassical features are predicted.

In this paper we report the experimental observation of the quantum effects of competing nonlinearities. We also report two clear classical signatures of competition: power clamping of the second harmonic and production of nondegenerate optical frequencies in both the second-harmonic and fundamental fields.

Figure 1 shows the conceptual layout. A frequency doubler, resonant at and pumped by a frequency ν, produces a nonresonant field of frequency 2ν which is forced to make a double pass through the cavity. The second harmonic can either downconvert back to the original mode, or act as the pump for the NDOPO. For the latter to occur the signal and idler modes ($\nu_{s,i} = \nu \pm \Delta$) must be simultaneously resonant with the mode ν. With sufficient power in the 2ν field the NDOPO can be above threshold, otherwise the system is below threshold and acts as an amplifier of the vacuum modes.

The three equations of motion for this system are

$$\dot{\alpha}_1 = -(\gamma_1 + i\Delta_1)\alpha_1 - 2\sqrt{\mu_1\mu_2}\,\alpha_1^*\alpha_s\alpha_i - \mu_1|\alpha_1|^2\alpha_1 + \sqrt{2\gamma_1^c}\,A_1,$$

$$\dot{\alpha}_{s,i} = -(\gamma_{s,i} + i\Delta_{s,i})\alpha_{s,i} - \sqrt{\mu_1\mu_2}\,\alpha_1^2\alpha_{i,s}^* - 2\mu_2\alpha_s\alpha_i\alpha_{i,s}^*, \tag{1}$$

where α_1, α_s, and α_i are the fundamental, signal, and idler field amplitudes, respectively; γ_x and Δ_x are, respectively, the decay rate and detuning of mode x; γ_1^c is the decay rate of the fundamental coupling mirror; μ_1 and μ_2 are the respective nonlinear interaction rates for SHG and NDOPO;
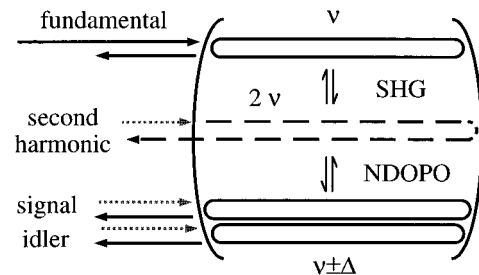

FIG. 1. Conceptual layout of the resonator. Dotted lines represent vacuum inputs, i.e., zero average power.

*FAX: +61(6) 2492747.
Electronic address: Ping.Lam@anu.edu.au

and $A_1 = \sqrt{P_1/(h\nu)}$, where P_1 is the pump power, h is Planck's constant, and ν is the fundamental frequency.

We define the term $\gamma_x^{\text{eff}} = (\gamma_x + i\Delta_x)$ as the effective decay rate of mode x. To see why, consider the case of a singly resonant frequency doubler ($\mu_2 = 0$). Without loss of generality, we can assume that the pump rate A_1 is real. If the detuning Δ_1 is zero, then the field value α_1 is real. It is clear that the value of α_1 is limited by the total decay rate γ_1: if γ_1 is large then the absolute value of α_1 will be small. Now consider nonzero detuning: the value of α_1 becomes complex and is limited by both the decay rate γ_1 and the detuning Δ_1. If the detuning is very large, then even when the decay rate is very small the absolute value of α_1 will be small. Thus the linear phase shift $i\Delta_1$ introduced by detuning leads to a reduction of intensity, and can be said to effectively increase the decay rate of the cavity.

For zero detunings, the threshold power for competition is

$$P_1^{\text{thr}} = h(2\nu)\frac{\overline{\gamma}}{\gamma_1^c}\frac{\gamma_1^2}{\sqrt{\mu_1\mu_2}}\frac{1}{4}\left(1 + r\frac{\overline{\gamma}}{\gamma_1}\right)^2, \qquad (2)$$

where $\overline{\gamma} = \sqrt{\gamma_s\gamma_i}$ and $r = \sqrt{\mu_1/\mu_2}$. We introduce the scaled power $N = P_1/P_1^{\text{thr}}$. For the likely experimental optimum, $\gamma_s = \gamma_i = \gamma_1$, $\mu_1 = \mu_2$, we define a minimum threshold power $P_1^{\text{min}} = h(2\nu)\gamma_1^2/(\eta\mu_1)$, where the cavity escape efficiency is $\eta = \gamma_1^c/\gamma_1$.

Obviously the threshold can be altered by changing the nonlinearities. Experimentally this is achieved via *phase matching*: i.e., altering the phase match in the nonlinear crystal by changing the orientation or temperature [4]. The threshold can also be altered via *dispersion matching*. That is, altering the laser frequency or cavity length so that the signal and idler modes are unable to be resonant with the fundamental. This corresponds to large signal and idler detunings but zero fundamental detuning. The altered threshold is then described by substituting absolute values of the effective decay rates, $|\gamma_x^{\text{eff}}|$, for all the decay rates in Eq. (2).

A detailed description of the experimental setup is given in [22]. In brief, the system is driven by a miniature diode pumped Nd:YAG ring laser (Lightwave 122) that produces a single mode of wavelength 1064 nm. A mode cleaning cavity acts as a low-pass filter to remove excess quadrature noise (both amplitude and phase) from the laser beam. The output of this drives the nonlinear cavity, which is a 12.5 mm long MgO:LiNbO$_3$ monolithic crystal with dielectric mirror coatings on the curved end faces ($R = 14.24$ mm). The monolith is singly resonant at the fundamental; the second harmonic executes a double pass through the crystal (residual second harmonic transmitted through the high reflector end is referred to as ''single pass''). The laser is locked to the monolith, and the mode cleaner is locked to the laser, via separate Pound-Drever locking schemes. The second harmonic is accessed via a low-loss dichroic, the reflected fundamental is accessed via the Faraday isolator — both beams are sent to either a balanced-homodyne pair and/or an optical spectrum analyzer.

The obvious signature of competition in this system is production of nondegenerate frequency modes (when $N > 1$). When the monolith is repeatedly scanned through resonance, these modes cause distorted cavity line shapes.
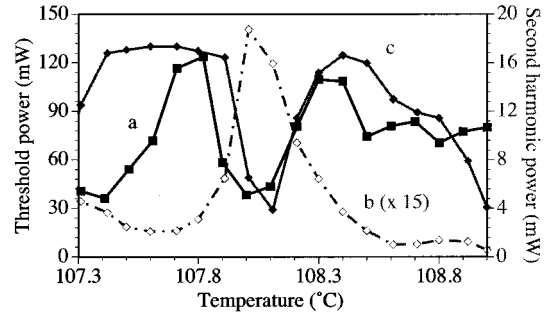

FIG. 2. (a) observed threshold power; (b) single-pass SH power (i.e., residual transmitted through high reflector), and (c) double-pass SH power (as shown in Fig. 1); as a function of crystal temperature (i.e., phase mismatch).

The frequency of the modes is measured by inspecting the infrared field reflected from the monolith with a spectrometer. The signal and idler pair are found to be up to 31 nm from degeneracy ($\nu_{s,i} = 1033$ nm, 1095 nm). The nondegeneracy is limited by phase matching, dispersion, and mirror bandwidth ($\sim$ 40 nm centered at 1064 nm). Figure 2 shows, for scanned operation [17], the observed threshold power (curve *a*) and the single-pass and double-pass second-harmonic power (curves *b* and *c*) as a function of the crystal temperature. Note that the threshold curve has two minima: roughly corresponding to maxima in the double-pass and single-pass power, respectively. In the latter case, even though minimal second-harmonic is produced, the intracavity second harmonic field is large enough to pump the NDOPO.

In locked operation the nondegenerate modes are observed via optical spectrum analyzers. Figure 3(a) is the output of the infrared optical spectrum analyzer for the laser only. Figure 3(b) is the output for the locked monolith just above threshold: note the strong conversion to signal and idler. The signal and idler mode hop irregularly, the system operating stably for up to ten minutes at a time. Gross control is achieved by detuning the fundamental mode. As it is detuned around resonance, the effective decay rate of the fundamental does not change greatly, but, due to dispersion
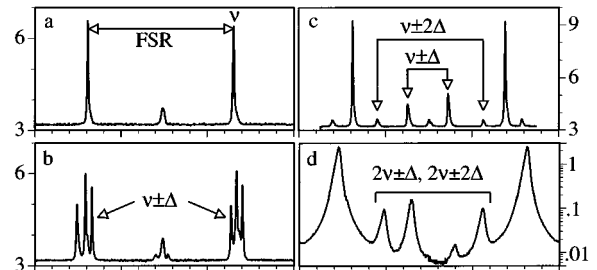

FIG. 3. Optical spectrum analyzer outputs of the locked monolith. All traces are intensity vs frequency (arbitrary units). The small peak in the middle of the infrared traces is due to imperfect alignment. *infrared traces* (a) from laser for $P_1 = 32$ mW, FSR = free spectral range of the analyzer; (b) from monolith for $P_1 = 14$ mW, note signal and idler modes; (c) from monolith for $P_1 = 49$ mW, note extra pair of modes; *visible trace* (d) from monolith for $P_1 = 155$ mW, the ordinate is logarithmic to highlight the four extra frequencies.

mismatch, the effective decay rates of the signal and idler can become very large. This shifts the threshold power above the operating power and suppresses the NDOPO cf. Eq. (2). Finer control has been achieved using a cavity with tunable dispersion, for example, a semimonolithic design where a translatable cavity mirror is external to the $MgO:LiNbO_3$ crystal [19]. Such improvements allow for stable operation with long intervals between mode hops.

Surprisingly, as the power is increased further two extra modes in the infrared, and four extra modes in the visible, are seen [Figs. 3(c) and 3(d)]. To the authors' knowledge this is the first observation of extra modes around the second harmonic, and it strongly supports the mechanism proposed in [15] of cascaded second-harmonic, sum, and difference frequency generation between the signal, idler, and pump fields. The extra modes in the visible light are likely generated by SFG ($\nu + \nu_{s,i} = 2\nu \pm \Delta$) or SHG ($2\nu_{s,i} = 2\nu \pm 2\Delta$), while the extra pair in the infrared are from DFG with the visible modes ($\nu + \nu_{s,i} - \nu_{i,s} = 2\nu_{s,i} - \nu = \nu \pm 2\Delta$). Further modes appear in the infrared field with increasing power: this system holds great promise both as a source of frequency tunable light and for frequency measurement (e.g., as a precise frequency chain).

Another surprising signature of competition is clamping of the second-harmonic power. From Eq. (1) we find that for $P_1 > P_1^{thr}$, the second-harmonic power is

$$P_2 = h(2\nu)\frac{\overline{\gamma}^2}{\mu_2}, \qquad (3)$$

i.e., the power is clamped to its threshold value. Above threshold, ''excess'' pump power is reflected or converted to signal and idler. Similar behavior has been predicted for the *optical limiter* [1]: a standing wave DOPO resonant at ν, which is single pass pumped at 2ν. The 2ν field in both cases sees three input-output ports, however the clamping is due to different mechanisms: competing $\chi^{(2)}$ nonlinearities in our system; cooperating $\chi^{(2)}$ nonlinearities in the limiter.

The conversion efficiency at threshold is given by $\epsilon = P_2/P_1^{thr}$. The minimum threshold, P_1^{min}, is the point of maximum conversion efficiency, with a value equal to the cavity escape efficiency $\epsilon = \gamma_1^c/\gamma_1 = \eta$. For unity cavity escape efficiency, $\eta = 1$, P_1^{min} is also the impedance matching point of the cavity.

Figure 4 shows experimental curves of second-harmonic versus fundamental power for two different detunings. In curve (a) the second-harmonic power is clamped at 23 mW at a threshold power of 41 mW. This threshold is much higher than the observed minimum threshold, $P_1^{min} = 14.3$ mW, as the signal and idler modes see high cavity losses due to dispersive mismatch. In curve (b) the monolith is tuned towards resonance so that the effective fundamental decay rate is lower than in curve (a), however the detuning increases the dispersive mismatch, and thus $\gamma_{s,i}$, suppressing the NDOPO and moving the threshold to 54 mW.

This has important consequences when designing nonlinear optical systems. Clamping is undesirable in many applications, such as frequency doubling to form a high power light source. With the development of low dispersion, efficient nonlinear cavities, clamping is expected to become a
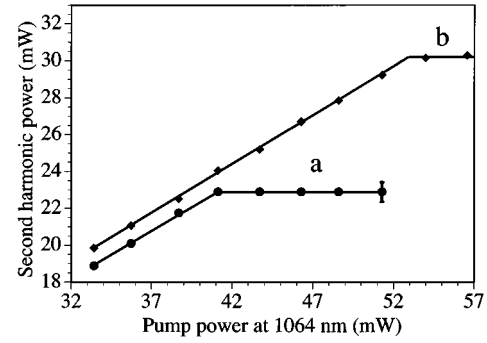

FIG. 4. Second-harmonic power vs fundamental power curves for two different detunings, (a) and (b). The systematic error bar is shown. All power measurements are NIST traceable with an absolute error of 7%.

widely observed phenomenon. In the past year alone it has been observed in systems with competing SHG and NDOPO [18–20] and in an optical limiter formed by an OPO intracavity with a laser [21]. It can be suppressed via tunable dispersion, or avoided entirely by designing the system so that the minimum threshold point occurs at a power higher than maximum pump power. Ideally clamping should not occur in many frequency doublers as they are optimized for maximum conversion efficiency, i.e., pumped at P_1^{min}. However in practice, many doublers are optimized by pumping them at powers above P_1^{min}. This is done because for powers less than P_1^{min} the conversion efficiency falls off very steeply: small variations in fundamental power lead to large variations in harmonic power. However, above P_1^{min} the conversion efficiency falls off very slowly: the harmonic power is much more robust to small variations in the fundamental power. It is exactly this regime which is prone to competition.

Naturally, competition also has quantum signatures. It has been suggested that, as the vacuum modes at $\nu_{s,i}$ are correlated by the NDOPO for $N < 1$, then competition could be observed as squeezing of the reflected pump field at detection frequencies around the difference frequency of the signal and idler, Δ [20]. In our experiment the free spectral range of the monolith, (which sets the minimum value of Δ), is much larger than the maximum bandwidth of the detectors (5.4 GHz and 100 MHz, respectively), ruling out any observation of this signature.

For the case where the second harmonic is resonant, the predicted quantum signature of competition is near perfect squeezing on either the fundamental or the second-harmonic mode in power regimes that are inaccessible in the absence of competition [16]. However, in our system the second harmonic is not resonant, and the quantum signature of competition is very different: above threshold the squeezing degrades. Without competition the second-harmonic squeezing spectrum is given by [22]

$$V_2 = 1 - \frac{8\gamma_{nl}^2 - 8\gamma_{nl}\gamma_1^c(V_1^{in} - 1)}{(3\gamma_{nl} + \gamma_1)^2 + \omega^2}, \qquad (4)$$

where the nonlinear loss rate, $\gamma_{nl} = \mu_1|\alpha_1|^2$; $\omega = 2\pi f$, where f is the detection frequency, and V_1^{in} is the amplitude
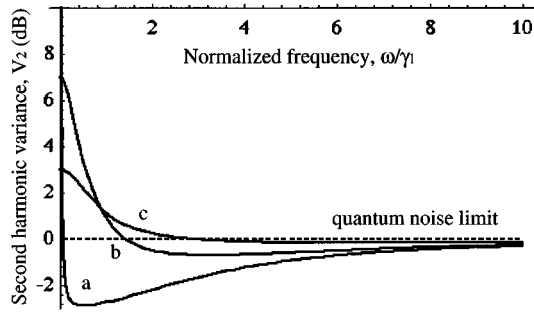
FIG. 5. Theoretical squeezing spectra for the case $P_1^{thr} = P_1^{min}$. (a) $N = 1.001$, (b) $N = 1.25$, and (c) $N = 3$.

FIG. 6. (a) Squeezing spectra. (a) Without competition, $P_1 = 74$ mW and (b) with competition, $P_1 = 60$ mW.

quadrature spectrum of the pump field. For $\gamma_{nl} \gg \gamma_1$ and $V_1^{in} = 1$ the maximum squeezing of $V = 1/9$ (-9.5 dB) is attained at zero frequency [23]. With competing nonlinearities the spectrum becomes

$$V_2 = 1 + \frac{2(N-1)B(\omega) - 2NA(\omega)}{(N-1)^2 B(\omega) + \omega^2 \left(\frac{\gamma_f}{2\,\overline{\gamma}}\right)^2 + \frac{C(N)NA(\omega)}{r} + \left(\frac{\omega^2}{2\,\overline{\gamma}}\right)^2},\quad (5)$$

where $N > 1$; $\gamma_f = \gamma_1 + r\,\overline{\gamma}$; $A(\omega) = r^2\omega^2$; $B(\omega) = \gamma_f^2 + \omega^2$; $C(N) = \gamma_1/\overline{\gamma} + r(N+1) + 2(N-1)$; and $V_1^{in} = 1$, $\gamma_1^c = \gamma_1$, for clarity. If we assume the minimum threshold for competition P_1^{min} then $\gamma_s = \gamma_i = \gamma_1$ and $\mu_1 = \mu_2$ and Eq. (5) simplifies to

$$V_2 = 1 + \frac{2(N-1-\hat\omega^2)}{4N^2\hat\omega^2 + (N-1-\hat\omega^2)^2},\quad (6)$$

where $\hat\omega = \omega/(2\gamma_1)$. A detailed theoretical discussion of the squeezing behavior under these simplified conditions is given in [24]. Maximum squeezing occurs at the point where competition begins. For the minimum threshold P_1^{min} the maximum squeezing is at zero frequency with a value $V = 1/2$ (-3 dB). For higher thresholds $P_1^{thr} > P_1^{min}$ the maximum squeezing is still at zero frequency, but with larger values. In all cases Eq. (6) connects to Eq. (4) without discontinuity.

As Fig. 5 shows, for $N > 1$ two effects come into play, both of which degrade the squeezing. Increasing N pulls the second-harmonic noise, at all frequencies, towards the noise of the second-harmonic input field. As this is a vacuum field, the noise is pulled towards shot noise, regardless of whether it was originally above (super-Poissonian) or below (sub-Poissonian) shot noise. Thus increasing N causes broadband degradation of the squeezing. This behavior is exactly analogous to that of an electro-optic noise eater, where increasing the beamsplitter reflectivity pulls the noise towards the limit set by the vacuum entering the empty beamsplitter port [25]. This noise eating behavior is expected to occur in other nonlinear optical systems: the optical limiter [26] and the saturated laser amplifier [27].

The additional squeezing degradation evident at low frequencies is due to a more subtle effect. In a conventional OPO, the signal and idler amplitude quadratures are very noisy above threshold (for a DOPO the amplitude is shot
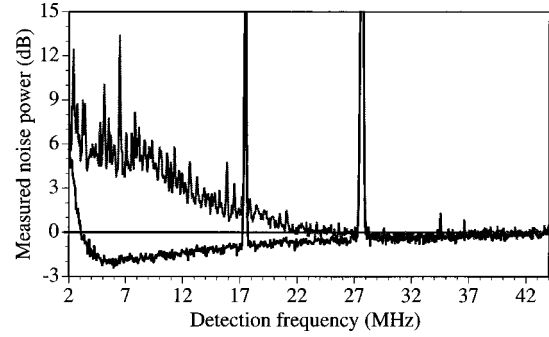
noise limited at $P = 4P_{thr}$ and 50% squeezed only for $P > 25P_{thr}$ [28]). This noise is transmitted to the amplitude of the second harmonic, degrading the squeezing. This low-frequency degradation decreases with increasing N (compare curves b and c in Fig. 5).

Figure 6(a) shows the experimentally observed squeezing in the absence of competition, which is suppressed via detuning as discussed earlier. Below 6 MHz the squeezing degrades due to laser pump noise [22], above 6 MHz the squeezing is as expected from theory with $V_1^{in} = 1$. The spikes at 17 and 27 MHz are from the locking signals. With competition, and at a lower pump power, the spectrum changes to that shown in Fig. 6(b). As predicted, there is considerable excess noise at low frequencies, while the degradation at higher frequencies is more gradual. The excess noise at low frequencies is greater than that shown in Fig. 5 due to the presence of numerous, overlapping, noise spikes. The spikes are due to a locking instability in the mode cleaner which is driven by competing locking signals. It is clear that even a small amount of $\chi^{(2)}$ competition leads to a marked degradation in the squeezing. This previously unexpected limit to squeezing can only be avoided by designing the system so that competition is suppressed when the pump power is greater than the maximum conversion efficiency power. One solution is a cavity with such high dispersion that the signal and idler modes are unable to become simultaneously resonant with the fundamental: high second-harmonic squeezing has been seen in such a system [29].

In conclusion, competition between SHG and NDOPO in a monolithic cavity has been observed to cause generation of new frequencies in both the visible and infrared fields, clamping of the second-harmonic power, and degradation of the second-harmonic squeezing. Competition imposes a previously unsuspected limit to squeezing and power generation. The reported signatures are expected to be commonly observed in efficient, low dispersion systems, unless explicit steps are taken to avoid competition.

[1] A. E. Siegman, Appl. Opt. **1**, 739 (1962).

[2] For example, see references in G. Assanto, G.I. Stegeman, M. Sheik-Bahae, and E. VanStryland, J. Quantum Electron. **31**, 673 (1995).

[3] G. Stegeman, M. Shei-Bahae, E. W. Van Stryland, and G. Assanto, Opt. Lett. **18**, 13 (1993).

[4] A. G. White, S. Schiller, and J. Mlynek, Europhys. Lett. **35**, 425 (1996).

[5] Z. Y. Ou, Opt. Commun. **124**, 430 (1996).

[6] P. L. Chu, B. A. Malomed, and G. D. Peng, Opt. Commun. **128**, 76 (1996).

[7] G. T. Moore and K. Koch, IEEE J. Quantum Electron. **29**, 961 (1993).

[8] E. C. Cheung, K. Koch, and G. T. Moore, Opt. Lett. **19**, 1967 (1994).

[9] K. Koch, G. T. Moore, and E. C. Cheung, J. Opt. Soc. Am. B **12**, 2268 (1995).

[10] R. Byer (private communication).

[11] S. Schiller and R. L. Byer, J. Opt. Soc. Am. B **10**, 1696 (1993).

[12] M. A. M. Marte, Phys. Rev. A **49**, 3166 (1994).

[13] G. T. Moore, K. Koch, and E. C. Cheung, Opt. Commun. **113**, 463 (1995).

[14] S. Schiller, G. Breitenbach, S. F. Pereira, R. Paschotta, A. G. White, and J. Mlynek, Proc. SPIE **2378**, 91 (1995).

[15] S. Schiller, G. Breitenbach, R. Paschotta, and J. Mlynek, Appl. Phys. Lett. **68**, 3374 (1996).

[16] M. A. M. Marte, Phys. Rev. Lett. **74**, 4815 (1995); M. A. M. Marte, Acta Phys. Slov. **45**, 253 (1995); M. A. M. Marte, J. Opt. Soc. Am. B **12**, 2296 (1995).

[17] The scanned measurements were performed by A.G.W. at Konstanz Universität, Germany using crystal No. 19.

[18] A. G. White, Ph.D. thesis, Australian National University, 1997 (unpublished).

[19] K. Schneider, G. Breitenbach, R. Paschotta, S. Schiller, and J. Mlynek (unpublished).

[20] J. Sorensen, E. Polzik, and J. Ostergaard (private communication).

[21] F. G. Colville, M. H. Dunn, and M. Ebrahimzadeh (unpublished).

[22] A. G. White, M. S. Taubman, T. C. Ralph, P. K. Lam, D. E. McClelland, and H.-A. Bachor, Phys. Rev. A **54**, 3400 (1996).

[23] R. Paschotta, M. Collett, P. Kürz, K. Fiedler, H.-A. Bachor, and J. Mlynek, Phys. Rev. Lett. **72**, 3807 (1994).

[24] S. Schiller, R. Bruckmeier, and A. G. White, Opt. Commun. (to be published).

[25] M. S. Taubman, H. Wiseman, D. E. McClelland, and H.-A. Bachor, J. Opt. Soc. Am. B **12**, 1792 (1995).

[26] M. Collett (unpublished).

[27] M. Gray (private communication).

[28] J. J. Slosser and G. J. Milburn, Phys. Rev. A **50**, 793 (1994).

[29] H. Tsuchida, Opt. Lett. **20**, 2240 (1995).